Trace Diffusion of Alkanes in Polyethylene: Spin-Echo Experiment and Monte Carlo Simulation

Ernst D. von Meerwall,*,†,‡ Heng Lin,† and Wayne L. Mattice†

Maurice Morton Institute of Polymer Science and Physics Department, The University of Akron, Akron, Ohio 44325-3909

Received December 8, 2006; Revised Manuscript Received January 25, 2007

ABSTRACT: We have performed pulsed-gradient NMR diffusion (D) measurements of five *n*-alkanes (24, 28, 36, 44, and 60 carbons) in a polyethylene (PE) host (molecular weight $M = 33$ kDa) as a function of concentration c (2−10 wt %) at 180 °C. Monte Carlo simulations on the second-nearest-neighbor diamond lattice (38, 46, 62, and 78 carbons) at c between 2% and 15% in a host of PE ($M = 4.5$ kDa) explored static and dynamic properties. The bridging method uses beads combining neighboring moieties and incorporates two-bead moves; it permits detailed reconstruction of the PE chain at any stage. It uses short-range rotational isomeric state and long-range intra- and interchain discretized Lennard-Jones potentials. For both experiment and simulation, trace D was obtained by extrapolating $D(c)$ to $c = 0$ using the Fujita−Doolittle model with known chain-end free-volume parameters. A single ratio of 330 Monte Carlo steps per picosecond brings simulation into excellent congruence with experiment; this factor is identical to that required for PE melts. The applicability of the Rouse model is approached only for the largest alkanes, but the resulting alkane M dependence of trace D is seen to be in transition from the Rouse-like M^{-1} dependence to a steeper value characteristic of reptation with constraint release. Since the M dependence of D for alkane melts adheres to a nearly linear $M^{-1.83}$ power law at this temperature, simulation and experiment confirm earlier theoretical considerations that the excess over M^{-1} arises entirely from the effects of the M-dependent host viscosity, or free volume, in the melts.

I. Introduction

The study of the diffusion of *n*-alkanes and polyethylene (PE) in the melt has consumed much experimental and theoretical effort.[1] Of particular interest in explaining the features of the observed molecular weight (M) and temperature (T) dependences has been the consequence of the strong dependence of alkane and PE density[2] on M and T. These density variations indicate a substantial free-volume fraction associated with chain ends,[3] known to have a sizable effect on the viscosity and the self-diffusion coefficient[4] D. In fact, the expected Rouse-like[5] dependence of D proportional to M^{-1} in alkanes is overwhelmed by free-volume effects, substantially steepened, so that the transition to entangled behavior expected in PE is obscured. Earlier investigators[6] found that D over a range of elevated temperatures was approximately consistent with an M^{-2} proportionality over the entire alkane−PE range; initial doubts about the applicability of the reptation-tube concepts[7] to PE were only slowly dispelled. More recently, precision measurements[2] of $D(M,T)$ in the liquid alkanes have guided the detailed theoretical modeling based on contemporary concepts of polymer dynamics; the model's success was based on the assumed underlying M^{-1} dependence of D. Molecular dynamics simulations[8] have reproduced the observations in considerable detail and further confirmed the theoretical interpretation. It should be pointed out that over most of the *n*-alkane series the conditions for the full applicability of the Rouse model are not yet satisfied,[9] but the intrinsic proportionality of D to M^{-1} appears to hold under more relaxed conditions.[10]

Diffusion measurements in PE melts[11] and in the related hydrogenated polybutadienes[12] have demonstrated an approach to the M^{-2} proportionality expected on the basis of the reptation/tube models in the high-M asymptotic limit, above the constraint release regime in the transitional M range near the entanglement onset molecular weight. Both theory[13] and simulations[14] have now successfully dealt with this transition. Two-component self-diffusion in binary blends of *n*-alkanes, and of *n*-alkanes with PE, has been measured[15] and simulated[16] as a function of concentration. These and binary blends of fully entangled PE of widely different M yield to analysis[17] based on extensions of the same theoretical model.

Simulations of the motions of chain molecules in a dense environment become increasingly arduous as M increases. Dynamic Monte Carlo (MC) methods offer the opportunity of extending the M range attainable without incurring massive computational effort. To be sure, MC methods lack an intrinsic time scale and must rely on comparison with experiment to establish this conversion, but given a fixed computational procedure a single conversion factor (e.g., number of MC steps per picosecond) will serve for a series of simulations over arbitrary ranges of M, concentration, and likely T as well. Representation of polymer chains in terms of connected beads deployed on a second-nearest-neighbor diamond (2nnd) lattice is a particularly felicitous choice for linear PE and its variants; this bridging method soon began to produce a body of results for both static and dynamic properties in monodisperse and polydisperse melts.[18,19] The recent inclusion of two-bead moves[9] has removed some minor remaining representational artificiality and has greatly reduced computational effort.

The removal of the free-volume host effect on self-diffusion in a series of homologous polymers is customarily performed in terms of a constant-free-volume correction based on the change of the glass transition temperature with M. A more direct procedure calls for measurements of trace amounts of each of a series of diffusants in a common host. Such measurements

* Corresponding author. E-mail: evonmee@uakron.edu.
† Maurice Morton Institute of Polymer Science.
‡ Physics Department.

10.1021/ma062819o CCC: $37.00
Published on Web 02/24/2007

have been performed, e.g., for the *n*-alkane series in rubbery host materials, with results consistent with a Rouse M dependence,[10] but the more easily interpreted measurements of trace D of *n*-alkanes in a PE host have to our knowledge never been reported. The present work was undertaken to remedy this omission, in order to examine the correctness of the underlying Rouse-like M dependence of D and to clarify the transition between unentangled and entangled diffusion. Both pulsed-gradient spin-echo diffusion experiments and dynamic MC simulations were employed.

Preliminary oral reports of this work have been given.[20]

II. Methods

A. Simulation. Dynamic NVT Monte Carlo simulations of the trajectories of *n*-alkane and PE chains were performed as described in detail elsewhere.[9] Briefly, chain molecules were represented as connected beads, each combining pairs of adjacent backbone carbon atoms with their linked hydrogens, and deployed in a high-occupancy second-nearest-neighbor diamond lattice in a way permitting unambiguous reconstruction of the real chain at any time. The size of the box with periodic boundary conditions varied with the system simulated; it always reproduced the experimental density of the system. Short-range potentials were rotational isomeric state model results, and long-range interactions assumed the Lennard-Jones form discretized for either two or three shells of neighbors. For static properties the contributions from the third shell could be safely neglected; their effect on cohesive energy was irrelevant as density was enforced to comply with experiment. However, there was a modest decrease in the simulated diffusion rate when the third shell was included. This effect is attributed to an increase in stickiness afforded by the extra attraction; thus, the results presented here include all three shells. The standard Metropolis algorithm at 180 °C governed the jumps of beads; a recently introduced repertoire of two-bead moves substantially increased computational efficiency and eliminated the need for postulating pivot moves. Following extended equilibration judged as attained after successfully passing three independent statistical tests, trajectory files were accumulated and later analyzed to obtain static and dynamic properties of the chains. Diffusion coefficients, including the laboratory-frame center-of-mass values desired for comparison with experiment, were extracted after testing for adherence to Fickian behavior and absence of artifacts. For the entire set of simulation conditions reported here, a single conversion factor relating the number of Monte Carlo steps to real-time units may be insisted upon and was determined by direct comparison with experiment (see below).

B. Samples. The *n*-alkanes used in the experimental part of this study were $C_{24}H_{50}$ (*n*-tetracosane), $C_{28}H_{58}$ (*n*-octacosane), $C_{36}H_{74}$ (*n*-hexatriacontane), $C_{44}H_{90}$ (*n*-tetratetracontane), and $C_{60}H_{122}$ (*n*-hexacontane). These were used as supplied by ICN Pharmaceuticals, K&K Lab (New York) (carbons 24, 28, and 36) or from Fluka Chemical Corp. (US) (carbons 44 and 60). In each case, the nominal purity of specimens was characterized as either *purum* (98%) or *puriss.* (99%). The polyethylene host material was obtained from Polymer Source, Inc. The supplier's characterization indicated a number-average molecular weight of 33 kDa and a dispersity index M_w/M_n of 1.05. In our diffusion experiments the neat alkanes showed no evidence of a diffusivity distribution, and the neat PE sample's modest D distribution was consistent with a log−normal M profile having the known polydispersity.

Low-concentration binary blends were made by weighing requisite aliquots of an alkane and PE, mixing these in powdered form where possible, inserting into 7 mm o.d. NMR sample tubes in amounts totaling between 200 and 300 mg and compacting mechanically. Sample tubes were flushed and filled with dry nitrogen and hermetically sealed. Concentration equilibration and elimination of bubbles required overnight heating to 150 °C. Diffusion measurements involved a 45 min exposure of samples to 180 °C including preheating. There was no evidence of thermal degradation.

C. Diffusion Experiment. For comparison with the simulation results and the calibration of the Monte Carlo time scale, experimental results for alkanes and melts were available from our earlier investigations of the *n*-alkane series[2] and for narrow-dispersity polyethylenes[11] and hydrogenated butadienes.[12] For the present work, new pulsed-gradient spin-echo diffusion measurements[21] were made at 180.5 °C of five alkanes (carbons 24, 28, 36, 44, and 60), each dissolved at five concentrations between 2 and 10 wt % in a polyethylene of $M = 33$ kDa. Our methods of making nonspectroscopic spin-echo diffusion measurements and interpreting the resulting data have been described in detail elsewhere.[22] Briefly, the three-pulse stimulated echo radio-frequency sequence was coordinated with a matched pair of pulsed magnetic field gradients of magnitude G and duration δ, separated by time Δ. Radio-frequency phase-sensitive detection of the echo signal recorded 3 kHz off-resonance was followed by Hamming-windowed magnitude Fourier transformation, integrating the peak area, and performing rms baseline correction. As a consequence of the gradient pulses, the spin echo in a diffusing substance is attenuated; here the amplitude was recorded as a function of pulse duration δ incorporated in a gradient parameter X (see eq 1). In this investigation, the parameter settings used were fixed values of $\Delta = 150$ ms, $G = 216$ G/cm, and a small steady gradient $G_0 = 0.3$ G/cm, with δ varied in 15−30 steps until the echo signal was attenuated to the background noise level or until 10 ms was reached. Echo height measurements were signal-averaged over 6−12 passes.

The diffusional echo attenuation was analyzed off-line by the current version of the Fortran code[23] DIFUS5K. The echo amplitude A was adequately reproduced by a two-component model of the form[21]

$$\frac{A(2\tau,X)}{A(2\tau,0)} = f_{\text{fast}} \exp[-\gamma^2 D_{\text{fast}} X] + (1 - f_{\text{fast}}) \exp[-\gamma^2 D_{\text{slow}} X] \tag{1}$$

where γ is the proton gyromagnetic ratio and

$$X = \delta^2 G^2 (\Delta - \delta/3) + \text{small correction terms in } GG_0$$

This model has three adjustable parameters: the two diffusion coefficients D_{fast} and D_{slow} and the relative echo amplitude f_{fast}. A slight improvement of the quality of the fit was possible. Because the polyethylene host material was modestly polydisperse, the single slow component was replaced by a disperse ensemble of rate components mapped onto the known M distribution[24] using reptational scaling, and D_{slow} was supplanted by $D(M_n)$, the reference diffusion coefficient of molecules of number-average mass. (A separate measurement in the neat PE sample confirmed this analysis of the slow component in the blends.) This improvement became increasingly important at the lowest concentrations, where the optimal extraction of the desired D_{fast} from the data at small f_{fast} most benefited from the accurate modeling of the slow component's echo attenuation. A sample echo attenuation plot with the fit of the modified eq 1 is shown in Figure 1a; particular attention was expended on the initial attenuation arising mainly from the fast-diffusing alkane (Figure 1b). The concentration dependence of $D(M_n)$ was, as expected, somewhat less than that of D_{fast}, and contributed no significant additional information, closely resembling the value recorded for the neat melt.

D. Theory for Melts and Blends. In unentangled *n*-alkane/polyethylene melts and blends, D_i of species $i = 1, 2$ was found to adhere to an expression depending on temperature T, molecular weights M_i, and volume fraction v_1, as follows:[2]

$$D_i(T,M_1,M_2,v_1) = A \exp(-E_a/RT) M_i^{-1} \exp[-B_d/f(T,M_1,M_2,v_1)] \tag{2}$$

in terms of a constant A, an intrinsic thermal activation energy E_a, a free volume overlap factor B_d, and fractional free volume f. In blends of homologous ingredients, as here, f must account for the chain-end free volume V_E in addition to a segmental contribution

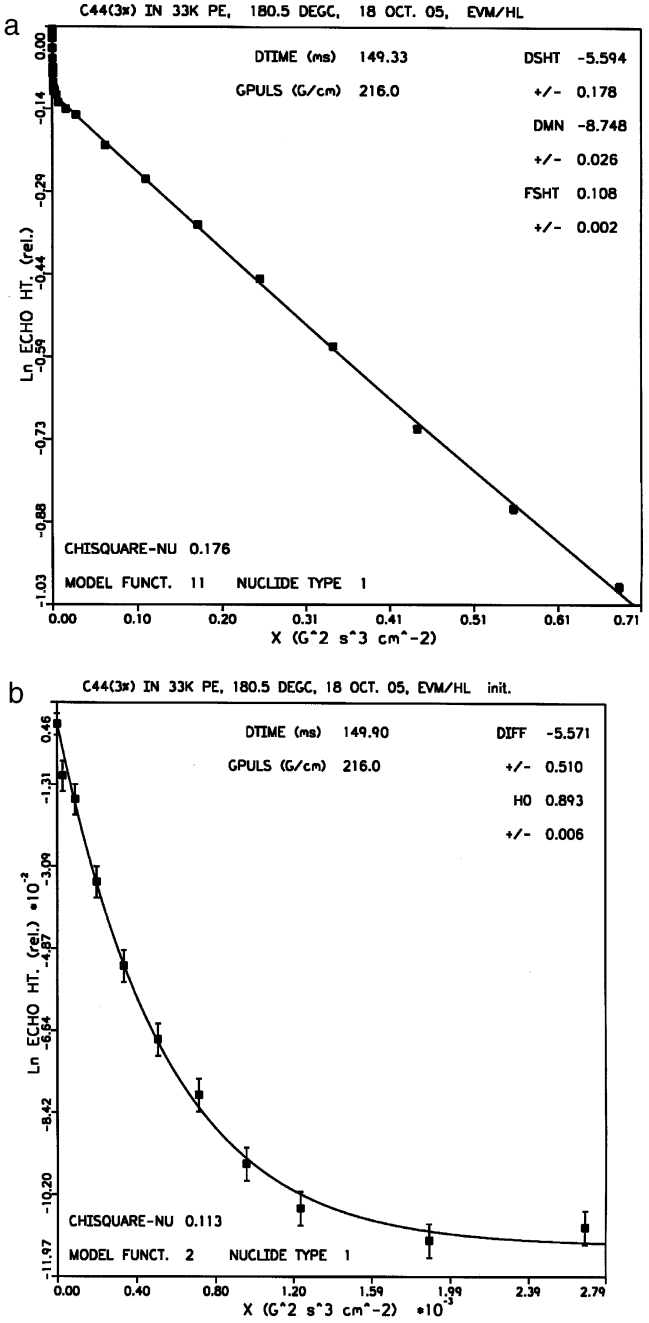

Figure 1. (a) Diffusional spin-echo attenuation at 180.5 °C in a blend of 3 wt % tetratetracontane in PE of $M = 33$ kDa (symbols). Line represents a successful three-parameter fit to the data of eq 1 modified to account for the PE component's measured M distribution. (b) Details of (a), displaying the initial echo attenuation due to the fast diffusion of the alkane component. Line represents fit of eq 1 to these data points only, with D_{slow} safely approximated as zero.

$f_\infty(T)$ present at all M:[3]

$$f(T,M_1,M_2,\upsilon_1) = f_\infty(T) + 2V_E(T)\,\rho[T, M^*(\upsilon_1)]/M^*(\upsilon_1) \qquad (3)$$

where $1/M^*(\upsilon_1) = \upsilon_1/M_1 + (1 - \upsilon_1)/M_2$.

In *n*-alkanes and PE the density ρ is a pronounced function of M and T, an effect which had been accurately modeled[2] on the basis of same free-volume parameters. If the heavier species begins to approach the entanglement ("ent") onset molecular weight M_c^0 in the melt, it was shown[15] that eq 2 was to be modified[12] to account for reptation ("rep") including constraint release ("CR")

$$D_i(\text{any } M) = [1/D_{Rouse} + 1/D_{ent}\,]^{-1} \qquad (4)$$

where $D_{Rouse} \sim M^{-1}$, $D_{rep} \sim M^{-2}$, $D_{ent} = D_{rep} + D_{CR}$, and $D_{CR} = \alpha D_{rep}\,(M_c/M)^2$ with $\alpha \approx 0.5$. The dilution of the entanglements of the heavy species by the lighter one may be accounted for by setting $M_c = M_c^0/(1 - \upsilon_1)^n$, $1 < n < 1.2$; blends with $M_c > M_2$ diffuse essentially unentangled. (For D_1 this modification affects only the interior of the concentration region and does not alter the results in melts or trace concentrations.) A further, approximate, refinement is, in general, necessary since as $\upsilon_1 \to 1$ the (unentangled) blend approaches a dilute solution of M_2 in solvent M_1; in such cases D_2 exhibits an M_2 exponent near -0.6 to -0.8. (This modification also did not come into play in the present work with its main attention to D_1.) This theory was evaluated for D_1 at $\upsilon_1 = 1$ for comparison with PGSE experimental results in melts and guided the assignment of an MC-step-to-time conversion factor for the melt simulation results. It was again evaluated for D_1 at $\upsilon_1 = 0$ for comparison with the results of the extrapolated trace diffusion measurements and simulations, discussed below.

E. Trace Diffusion. The principal reason for measuring or simulating trace diffusion coefficients is the elimination of any molecular weight dependence of the host effect which complicates the interpretation of diffusion in series of melts. Trace diffusion of an homologous series of diffusants in an identical host provides unambiguous information about the M-dependent evolution of diffusion mechanisms of single molecules, e.g., during the change from unentangled to entangled translational motion.

Using the lowest concentrations for which precise two-component diffusion results are possible can already distort the results, e.g., of the M dependence of "trace" diffusion. Thus, trace D is not directly obtainable from either experiment or simulation but must rely on an extrapolation to infinite dilution of determinations at several low concentrations.[10] In order to reduce the scatter and uncertainty in these extrapolations particularly at the lowest concentrations, it was decided to guide the fits by supplying a reliable constraint to each concentration dependence, leaving only the intercept freely adjustable. The weight fraction (w_1) dependence of D_1 for species 1 diffusing in an homologous species 2 may be expressed by combining the Fujita−Doolittle expression[25] applicable to binary blends[10] with chain-end free-volume considerations according to Bueche,[3] as follows:

$$\log D_1(w_1,M_1,T) = \log D_1(0,M_1,T) + (sw_1)/[2.303(1 + sf_2w_1)\,] \qquad (5)$$

where $s = \Delta f/f_2^2$, $f_2(T,M_2) = f_{2\infty}(T) + 2V_E(T)\rho(T,M_2)/M_2$, $\Delta f\,(T) = 2V_E(T)[1/M_1 - 1/M_2\,]$, and $\rho(T,M_2) = [1/\rho_\infty(T) + 2V_E(T)/M_2\,]^{-1}$. In the limit of zero concentration, the (initial) slope of log D_1 vs w_1 is $s/2.303$.

From previous work on the alkane−PE melt series[2,15] the values of the high-M free-volume fractions $f_\infty(T)$, densities $\rho(T,M)$, and chain-end free volumes $V_E(T)$ were available at arbitrary T and M. Using these, trace $D_1 = D_1(0,M_1,T)$ was obtained from a one-parameter fit to the data log D_1 vs w_1 at fixed $T = 180$ °C.

III. Results and Discussion

A. Simulation. The simulations, among much other information available from the trajectory files, provided center-of-mass diffusion coefficients at concentrations at and below 15 wt %. For octatriacontane and hexatetracontane three concentrations were simulated, the lowest being 5 wt %; for dohexacontane and octaheptacontane four concentrations were simulated, the lowest either 2 or 2.4 wt %.

Practical considerations dictated an effective lower limit near 38 carbons for the size of the trace alkane, in keeping with the precision required for the analysis at the lowest acceptable trace concentrations. The desirable full overlap in molecular weight ranges of simulation and experiment was therefore not possible. Similar practical constraints, related to computing effort, also confined the simulations to a box size smaller than necessary to accommodate the host M of 33 kDa as used in the

Table 1. Simulated and Measured Trace Diffusion of *n*-Alkanes in PE

	slope parameter s^a		
n-alkane	simulation	experiment	log D(trace) (cm^2/s)
$C_{24}H_{50}$		2.19	-5.38 ± 0.02
$C_{28}H_{58}$		1.87	-5.45 ± 0.02
$C_{36}H_{74}$		1.45	-5.53 ± 0.02
$C_{38}H_{78}$	1.38		-5.58 ± 0.03^b
$C_{44}H_{90}$		1.19	-5.66 ± 0.02
$C_{46}H_{94}$	1.14		-5.68 ± 0.03^b
$C_{60}H_{122}$		0.86	-5.83 ± 0.02
$C_{62}H_{126}$	0.84		-5.83 ± 0.03^b
$C_{78}H_{158}$	0.66		-6.07 ± 0.03^b

[a] Derived from *n*-alkane melt data analysis (ref 2) via eq 5. [b] Applying conversion factor of 330 MC steps/ps.

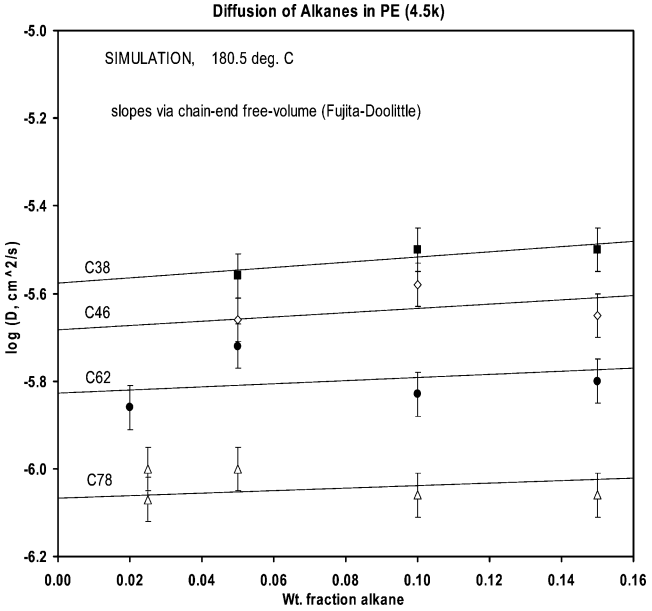

Figure 2. Results of the dynamic MC simulations of center-of-mass diffusion of four *n*-alkanes at several low concentrations in a monodisperse PE host of 4.5 kDa (symbols). Ordinate scale is based on a conversion of 330 MC steps/ps. Trace diffusion coefficients are the zero-concentration intercepts of the one-parameter fits to the data (lines) of eq 5 based on literature values of free-volume parameters for the *n*-alkane series.

experiments. Thus, the host PE was given a molecular weight of 4.5 kDa, still much higher than the entanglement onset molecular weight M_c. Inspection of eqs 2−4 shows that this difference in host M has only minimal influence on D_{fast} and hence on trace diffusion as extrapolated by fitting the intercept in eq 5 to the data. The fixed slope parameter s in eq 5 and the fitted trace D are given in Table 1; concentration-dependent data and fits are shown in Figure 2. Conversion of simulation steps to real time was taken from earlier experiments[9] on melts; the ratio used was 330 MC steps/ps and was retained for the trace simulations. This conversion had been performed iteratively using several trial values of this ratio, selecting the interpolated value for which the agreement of the scaled simulations with PGSE melt experiments was visually optimal over the full range of overlap; no numerical fitting was performed.

B. Experiment. Diffusion coefficients in the binary alkane−PE blends at each of four or five alkane concentrations between 2 and 10 wt % were obtained from the experimental diffusional echo attenuation data as described above and exemplified in Figure 1a,b. The host PE had a nominal $M_n = 33$ kDa and a dispersity ratio 1.05. The extraction of D_{fast} from echo attenuation data particularly at the lowest concentrations depends crucially on the correctness of the modeling of the initial attenuation of the slow component echo. Close examination of the echo attenuation in the neat 33 kDa melt showed no evidence of a rapidly diffusing species or contaminant (e.g., solvent residue; oligomers); the log−normal M distribution used in the modeling[24] of the echo attenuation was in excellent agreement with the data in the melt and, with the addition of a fast component, in all the binary blends. The corresponding host D distribution is barely detectable as a small upward concavity in the final slope in Figure 1a. The echo amplitude fraction arising from the fast component is not necessarily a good check on the correctness of the separation between echo contributions: the fast component is usually preferentially T_2-weighted, larger than the corresponding mass fraction. This effect is substantial in the present work for all blend data. But whereas both D_{fast} and $D(M_n)$ were precisely extractable, the latter proved uninformative for our purposes, increasing slightly from log $D(M_n) = -8.75 \pm 0.02$ at 2 wt % alkane (also the value measured in the neat PE) to -8.69 ± 0.02 at 10%, independent of alkane species within the attainable precision. Figure 3 shows the measured diffusion coefficients D_{fast} together with constrained fits of eq 5 for direct comparison with the simulation results, included in Table 1.

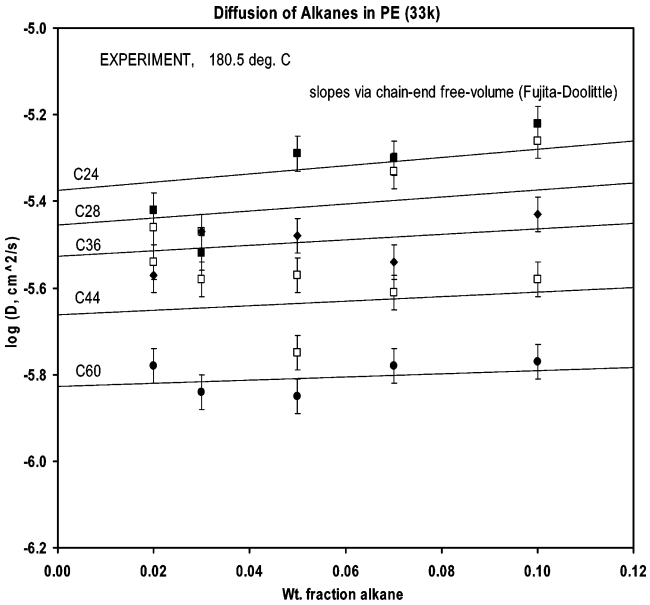

Figure 3. Results of the pulsed-gradient spin-echo diffusion measurements of D_{fast} in five *n*-alkanes at several low concentrations in a moderately disperse PE host of 33 kDa (symbols). Trace diffusion coefficients are the zero-concentration intercepts of the one-parameter fits to the data (lines) of eq 5 based on literature values of free-volume parameters for the *n*-alkane series.

C. Trace and Melt: Comparison. The results for trace diffusion simulation and experiment from the present work have been collected together with those of earlier work in *n*-alkane,[2] PE,[9,11] and hydrogenated polybutadiene[12] melts and are presented in the master plot of Figure 4. Also shown are evaluations of the theory of eqs 2−4, with parameters determined in earlier studies. No further fitting was performed. Experimental PE melt diffusion measurements (earlier work) had been performed at 175 °C; alkane diffusion was extrapolated from 170 to 175 °C using the accurately known activation energies; all melt and trace simulations and trace experiments were performed at 180 °C; and all theory was evaluated at 178 °C. Several observations are in order.

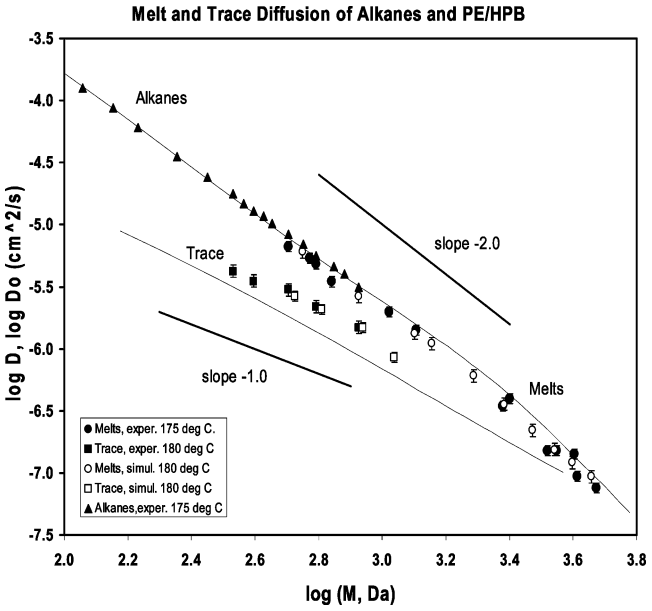

Figure 4. Molecular weight dependence of diffusion in alkane and PE melts (literature) and of trace alkanes in PE (present work, Figures 2 and 3). Experiment (solid symbols) and simulation (open symbols) are related through a single conversion factor. Thin lines represent theory of eqs 2−4 evaluated for melt D and for trace D in a PE host of $M_2 = 5$ kDa.

In the melts, experiment and scaled simulation[9] share a common M dependence over the entire domain of overlap. This M dependence is closely reproduced by the theory of eqs 2−4 with parameters derived in earlier work. The power-law slope of log D vs log M is near −1.8 for the alkanes at this temperature, displays a small inflection in the transitional region centered on $M_c \approx 1500$, and then assumes a value near −2.4 up to $M = 5000$. These and other experimental studies[26,27] have shown that the slope then flattens, approaching a limiting value only slightly steeper than −2.0, in at least semiquantitative agreement with evaluations of the theory described here.

In the present trace diffusion study, experiment and theory again share a common M dependence over the small available domain, whose extent is limited on the experimental side by the lack of alkanes with carbon numbers above 60, and in the simulations by the lessened reliability of results for short chains as well as by computational effort for long chains dilutely dissolved in blends. The agreement seen in the overlap domain is attained without altering the melt-derived conversion factor between Monte Carlo steps and units of real time.

The melt and trace data diverge increasingly at low M. In fact, the slope in Figure 4 for the set of all experimental and simulation trace data for $M < 1000$ is consistent with −1.0, in excellent agreement with the underlying Rouse-like diffusion mechanism expected, and included in the theory.

An evaluation of the full theory in its trace D mode ($v_1 = w_1 = 0$) is also shown. Its results lie somewhat below the data but display an M-dependent trend in rough agreement with the data. Significantly, a slope of −1 is not approached by the theory until M_1 is well below 20 carbons. Any disagreement between theory and simulation/experiment is not due to the choice of the host $M = M_2$ or their difference between experiment and simulation. The figure shows an evaluation for $M_2 = 5.0$ kDa, but the results over the data domain do not differ significantly if $M_2 = 33$ kDa is used instead. Those differences only become evident above $M_2 \approx 2$ kDa, well outside the region of interest here. Of course, the trace theory smoothly joins the melt theory near $M_1 = M_2$, as required.

Equally significantly, it is evident from the combination of experiment, simulation, and theory at trace concentrations in a common host that the approach to laterally constrained motion, and the transition to fully entangled diffusion,[28] is far more gradual and more subtle than suggested by the customary invocation of limiting power-law slopes of −1 and −2 meeting at $M = M_c$. This subtlety greatly reinforces that evident from the better known melt results. But whereas trace diffusion studies remove the obscuring influence of the changing free volume in melt studies, they do not entirely obviate the other main disturbance in the transition to strict reptation. Inspection of eqs 2−4 suggests that the diffusion-enhancing effects of constraint release depend sensitively not only on M_1 but also on M_2 well beyond $M = M_c$. The influence of contour length fluctuations on diffusion[29] is still not clearly understood[26] but is likely to be smaller[30] than its effect on the viscosity. This mechanism has been ignored in the theory evaluated in the present study.

IV. Summary and Conclusion

In the immediate predecessor work a dynamic Monte Carlo algorithm had been constructed, incorporating random local two-bead moves, and applied to the study of polyethylene chains in the vicinity of the entanglement transition. It had efficiently generated expected and plausible results, e.g., anomalous segment behavior for shorter chain lengths, Rouse dynamics of single chains, and anomalous diffusion of the center of mass at short times. This algorithm was used here to investigate the self-diffusion of entangled linear PE molecules as well as of several *n*-alkanes at small concentrations in the entangled PE host.

Extrapolation to infinite dilution was performed to obtain trace diffusion coefficients, with results compared to experiment using the pulsed-gradient spin-echo NMR method.

The center-of-mass diffusion coefficients in melts and in trace alkanes are found to be in agreement with experiment, using a common scaling factor relating Monte Carlo steps to real time. The transition from unentangled to entangled diffusion is seen to be quite gradual, centered on M_c near 1.5 kDa, where relaxation time still shows intermediate behavior.

The theory developed in connection with our earlier diffusion studies of alkane and PE melts and in binary *n*-alkane−PE blends somewhat underpredicts the extrapolated trace diffusion results in the present work. However, it adequately reproduces the M-dependent trend in the observed and simulated results. It also clearly reveals the very gradual transition between unentangled and fully entangled diffusion.

The present work will be augmented to improve our understanding of this transition by widening the M range of the trace alkane component in PE. Other concurrent work[31] investigates polydispersity effects on polymer dynamics using bidisperse systems. Additional information may be obtained by studying diffusion of both components in bimodal blends across the full concentration range.

Acknowledgment. The authors thank Dr. N. Waheed for assistance with the diffusion measurements, several helpful suggestions, and his critical review of the manuscript. We gratefully acknowledge support of this work by NSF through Grants DMR 00 98321 and DMR 04 55117 and by the Ohio Board of Regents.

References and Notes

(1) See, for example: Ertl, H.; Ghai, R. K.; Dullien, F. A. L. *AIChE J.* **1974**, *20*, 1 and literature cited therein.
(2) von Meerwall, E.; Beckman, S.; Jang, J.; Mattice, W. L. *J. Chem. Phys.* **1998**, *108*, 4299.
(3) Bueche, F.; Kelley, F. N. *J. Polym. Sci.* **1960**, *45*, 267.
(4) von Meerwall, E.; Grigsby, J.; Tomich, D.; Van Antwerp, R. *J. Polym. Sci., Polym. Phys. Ed.* **1982**, *20*, 1037.
(5) Rouse, P. E. *J. Chem. Phys.* **1953**, *21*, 1272.
(6) Fleischer, G. *Colloid Polym. Sci.* **1986**, *264*, 1.
(7) de Gennes, P.-G. *J. Chem. Phys.* **1971**, *55*, 572; *Macromolecules* **1976**, *9*, 587 and 594.
(8) Harmandaris, V. A.; Doxastakis, M.; Mavrantzas, V. G.; Theodorou, D. N. *J. Chem. Phys.* **2002**, *116*, 436.
(9) Lin, H.; Mattice, W. L.; von Meerwall, E. D. *J. Polym. Sci., Part B: Polym. Phys.* **2006**, *44*, 2556.
(10) von Meerwall, E. D.; Ferguson, R. D. *J. Appl. Polym. Sci.* **1979**, *23*, 877.
(11) Pearson, D. S.; VerStrate, G.; von Meerwall, E.; Schilling, F. C. *Macromolecules* **1987**, *20*, 1133.
(12) Pearson, D. S.; Fetters, L. J.; Graessley, W. W.; VerStrate, G.; von Meerwall, E. *Macromolecules* **1994**, *27*, 711.
(13) Graessley, W. W. *Adv. Polym. Sci.* **1982**, *47*, 68.
(14) Harmandaris, V. A.; Mavrantzas, V. G.; Theodorou, D. N.; Kröger, M.; Ramirez, J.; Öttinger, H. C.; Vlassopoulos, D. *Macromolecules* **2003**, *36*, 1376.
(15) von Meerwall, E.; Feick, E. J.; Ozisik, R.; Mattice, W. L. *J. Chem. Phys.* **1999**, *111*, 750.
(16) Harmandaris, V. A.; Angelopoulou, D.; Mavrantzas, V. G.; Theodorou, D. N. *J. Chem. Phys.* **2002**, *116*, 7656.
(17) von Meerwall, E.; Wang, S.; Wang, S.-Q. *Polym. Prepr.* **2003**, *44*, 287.
(18) Rapold, L.; Mattice, W. L. *Macromolecules* **1996**, *29*, 2457. Cho, J.; Mattice, W. L. *Macromolecules* **1997**, *30*, 637. Doruker, P.; Mattice, W. L. *Macromolecules* **1997**, *30*, 5520.
(19) Clancy, T. C.; Mattice, W. L. *J. Chem. Phys.* **2000**, *112*, 10049. Xu, G.-Q.; Mattice, W. L. *J. Chem. Phys.* **2002**, *117*, 3440. Ozisik, R.; von Meerwall, E.; Mattice, W. L. *Polymer* **2002**, *43*, 629.
(20) von Meerwall, E.; Lin, H.; Mattice, W. L. *Bull. Am. Phys. Soc.* **2006**, *51*, 1572; *Bull. Am. Phys. Soc.*, in press.
(21) Tanner, E. O.; Stejskal, J. E. *J. Chem. Phys.* **1965**, *42*, 288.
(22) Current, practices of this laboratory are described in: Iannacchione, G.; von Meerwall, E. *J. Polym. Sci., Part B: Polym. Phys. Ed.* **1991,** *29*, 659. Pacanovsky, J.; Kelley, F. N.; von Meerwall, E. *J. Polym. Sci., Part B: Polym. Phys. Ed.* **1994**, *32*, 1339. Oh, J. S.; Isayev, A. I.; von Meerwall, E. *Rubber Chem. Technol.* **2004**, *77*, 745.
(23) von Meerwall, E. D.; Ferguson, R. D. *Comput. Phys. Commun.* **1981**, *21*, 421.
(24) von Meerwall, E.; Palunas, P. *J. Polym. Sci., Polym. Phys. Ed.* **1987,** *25*, 1439.
(25) Fujita, H. *Fortschr. Hochpolym.-Forsch.* **1961**, *3*, 1.
(26) Wang, S. *J. Polym. Sci., Part B: Polym. Phys.* **2003**, *41*, 1589.
(27) Tao, H.; Lodge, T.; von Meerwall, E. D. *Macromolecules* **2000**, *33*, 1747.
(28) This subject is extensively reviewed in: McLeish, T. C. B. *Adv. Phys.* **2002**, *51*, 1379.
(29) Frischknecht, A.; Milner, S. *Macromolecules* **2000**, *33*, 5273.
(30) Wang, S.; von Meerwall, E.; Wang, S.-Q.; Halasa, A.; Hsu, W. L.; Zhu, J. P.; Quirk, R. P. *Macromolecules* **2004**, *37*, 1641 and references cited therein.
(31) Lin, H.; Mattice, W. L.; von Meerwall, E. D. *Macromolecules* **2007**, *40*, 959.

MA062819O